

EFFECT OF CADMIUM-TERBIUM SUBSTITUTION IONS ON DIELECTRIC PROPERTIES OF $Mg_{0.5-x}Cd_xCo_{0.5}Cr_{0.04}Tb_yFe_{1.96-y}O_4$ FERRITES

G. MUSTAFA*, M.UL ISLAM

Department of Physics, Bahauddin Zakariya University Multan 60800, Pakistan

A series of $Mg_{0.5-x}Cd_xCo_{0.5}Cr_{0.04}Tb_yFe_{1.96-y}O_4$ (with $0 \leq x \leq 0.5$ and $0 \leq y \leq 0.10$) ferrites has been synthesized by sol-gel auto combustion method. The synthesized samples were characterized using thermal (TGA/DTA) and morphological (SEM/EDX). The dielectric properties of these were also carried out. The decrease of permittivity with the increase of frequency in the range of 1MHz to 3GHz follows the Maxwell-Wagner model. Moreover, the (Cd^{2+} , Tb^{3+}) partial substituted ions have smaller values of loss tangent and dielectric constant which is favorable for the applications where low losses are desired. The value of ac conductivity increased with an increase in the frequency and decreased with substitution of Cd^{2+} and Tb^{3+} which reflects the hopping mechanism due to electron of exchange Fe^{2+} and Fe^{3+} at respective sites and also small polaron of divalent cations. Electric module of the presented sample showed semicircle attribution to the grain boundary effect. Such materials are considered as electromagnetic attenuation materials, suitable for switching and microwave devices.

(Received April 8, 2019; Accepted August 3, 2019)

Keywords: Spinel ferrite, Sol-gel, TGA/DTA, Drift mobility, AC conductivity

1. Introduction

The properties of ferrimagnetic materials are tailored by adding divalent or trivalent ions of suitable valences with appropriate thermal treatments [1]. Such materials are commonly used in the area of applications such as microwave absorption materials due to their low complex permittivity and high values of DC resistivity [2]. The dielectric constant normally interprets the amount of the dissipated electrical energy which is affected by several factors such as the electrical conduction, dielectric relaxation, and resonance losses of dielectric, variation thickness of the layer that absorbs the microwaves and the nonlinear processes. For the superior performances and efficiency, noise and dielectric losses should be minimize. Dielectric losses increase due to many reasons one of them may be the absorption of moisture in the pores of the synthesized sample. It shows the importance of porosity of the dielectric material [3]. Rezsescu et al [4] investigated the effects of substitution of different types and amounts of rare earth ions on the ferrite structures along with their change in electromagnetic properties. The unpaired electrons of rare earth ions have strong spin-orbit coupling 4f-3d and angular momentum. Kolekar et al [5] reported that the cadmium doped spinel ferrites have high resistivity. Since last few decades many researchers have been showing their great interest and reporting about the substitution of divalent and trivalent (including rare earth) ions in the spinel ferrites [6] for high-frequency applications. In the present case, the substituted (Cd^{2+} , Tb^{3+}) ions have larger ionic radii, therefore the occupancy of these ions into the spinel lattice would possibly create a lattice distortion and it is expected that all the material properties may modify to an appreciable extent. The properties of these compounds depend upon the nature and radii size of the substitutions along with the cooperative behavior of such cations. There are many factors which can put influence on the characteristics of the ferrite materials such as their synthesizing routes, chemical composition, sintering temperature and time duration of sintering process. Even that rate of flow of heat and cooling during and after sintering is also considered an important parameter. Researchers have been taking great interest in auto-combustion sol-gel process since last decade. This protocol makes best quality homogeneous and

*Corresponding author: ghulammustafabzu@gmail.com

nano-sized material at low temperature as compared to other protocols. In this work, we are focusing to investigate the role of co-substitution ions of larger ionic radii of divalent and trivalent cations (Cd^{2+} , Tb^{3+}) on the dielectric response of $\text{Mg}_{0.5-x}\text{Cd}_x\text{Co}_{0.5}\text{Cr}_{0.04}\text{Tb}_y\text{Fe}_{1.96-y}\text{O}_4$ ferrites. The values of resistivity and permittivity loss factor are considered as control elements for attaining the desired materials. The acquired values of resistivity and permittivity loss factor among synthesized materials are used in many electronic devices.

2. Experimental procedure

Spinel ferrites with chemical formula $\text{Mg}_{0.5-x}\text{Cd}_x\text{Co}_{0.5}\text{Cr}_{0.04}\text{Tb}_y\text{Fe}_{1.96-y}\text{O}_4$ (with $x = 0$ to 0.5 in steps of 0.1 and $y = 0.00$ to 0.10 in steps 0.02) were successfully synthesized by Sol-gel auto combustion technique. In this method, best quality chemicals of analytical grade were being used: $\text{Mg}(\text{NO}_3)_2 \cdot 6\text{H}_2\text{O}$, $\text{Cd}(\text{NO}_3)_2 \cdot 6\text{H}_2\text{O}$, $\text{CoCl}_2 \cdot 6\text{H}_2\text{O}$, $\text{Cr}(\text{NO}_3)_3 \cdot 6\text{H}_2\text{O}$, Tb_2O_3 , FeCl_3 and citric acid $\text{C}_6\text{H}_8\text{O}_7 \cdot \text{H}_2\text{O}$. The sol-gel method which described as earlier reported in the elsewhere [7]. The gel like material was then grinded after drying it in order to get sample in powder form. Pellets of these samples having thickness of 0.3 cm were made using hydraulic press (Paul-Otto) by applying 35 kN load and sintered at a temperature of 900°C for 8 h. in order to get pallets with smooth surface, these were polished. Surface morphology was studied via Scanning electron microscope (SEM) model JSM-6490 JEOL. Thermal behavior of the prepared samples was analyzed via thermogravimetric analysis and differential thermal analysis (TGA/DTA). An Agilent impedance / materials analyzer model E4991ARF, with the 16453A test fixture was used for dielectric measurements at room temperature and frequency range was 1MHz - 3GHz .

2.1. Characterization

The two-probe method was employed to measure the DC electrical resistivity of spinel ferrites at room temperature. This was done with the use of a source meter model (Keithly-197). Following equation was used to measure the DC resistivity of each sample;

$$\rho = \frac{RA}{d} \quad (1)$$

(where $A = \pi r^2$ and $R = \frac{V}{I}$); in the above relation ‘‘R’’ represents the ‘‘A’’ sample resistance whereas ‘‘d’’ denotes for thickness as well as the area of pellets. To calculate the Drift mobility of spinel ferrites from measure resistivity, we use the following relation;

$$\mu_d = \frac{1}{ne\rho} \quad (2)$$

Here ‘‘e’’ denotes the charge of the electron, ‘‘n’’ represents charge contents carrier. The ‘‘n’’ was measured by the given expression:

$$n = \frac{N_A \rho P_{\text{Fe}}}{\text{Molecular weight}} \quad (3)$$

where N_A Avogadro number, ρ_m represents the samples’ bulk density, P_{Fe} represents the iron atoms numbers of specified formula whereas ‘‘M’’ represents the symbolical expression of sample’s molecular weight. Different parameters as dielectric constant ϵ' , Ac conductivity and dielectric loss ($\tan \delta$) were calculated with the help of impedance analysis after this resultant quantities were measured by using the following expression [8];

$$\epsilon' = \frac{C_o}{C_p} \quad \text{where } C_o = \frac{A \epsilon_0}{d} \quad (4)$$

$$\tan \delta = \frac{1}{\omega C_p R_p} \quad (5)$$

$$\sigma_{ac} = \omega \epsilon_0 \epsilon' \tan \delta \quad (6)$$

where C_o is the capacitance of sample in vacuum attributed to the d spacing of electrode and the A area of electrode, the applied field angular frequency ω and ϵ_0 calculated permittivity in vacuum. C_p denoted to the electrical equivalent ferrite sample taken in capacitor form. The impedance have real as well as imaginary parts which can verify by applying the impedance absolute $|Z|$ with different complex angle θ_z can be measured by these relations:

$$Z' = R = |Z| \cos \theta_z \quad (7)$$

$$Z'' = R = |Z| \sin \theta_z \quad (8)$$

The electrical modulus have real and imaginary components represented M' and M'' [9]:

$$M_r'(\omega) = \frac{\epsilon_R}{(\epsilon_R(\omega)^2 + \epsilon_I(\omega)^2)} \quad (9)$$

$$M_i''(\omega) = \frac{\epsilon_I}{(\epsilon_R(\omega)^2 + \epsilon_I(\omega)^2)} \quad (10)$$

where ϵ_R , real and ϵ_I imaginary parts of the permittivity.

3. Results and discussion

Detailed structural analysis was fully determined by XRD data as a functions of x were interpreted in the previous reported work [7]. Thermal gravimetric analysis (TGA) and differential thermal analysis (DTA) is an important tool for studying the thermal dynamic nature of solid materials. The evolution in structural phase in solid material is studied with this technique. Fig. 1 shows the representative samples of TGA/DTA curves with different $(x,y) = (Cd^{2+}, Tb^{3+})$ contents such as sample A denoted by $(x, y) = (0.2, 0.04)$, sample B $(x, y) = (0.1, 0.02)$ and sample C denoted $(x, y) = (0, 0)$ respectively. The observation about weight losses (%) versus increasing temperatures appears in step around room temperature to $100^\circ C = 22\%$, $100^\circ C - 210^\circ C = 7\%$, $210^\circ C - 630^\circ C = 27\%$, $630^\circ C - 690^\circ C = 15\%$ and $690^\circ C - 1000^\circ C = 9\%$ respectively. In the first interval about 22% weight losses of the prepared sample, it could be due to removal of water while $100^\circ C - 210^\circ C = 7\%$ is due to the excretion of excess deposited water. In range $630 - 690^\circ C = 15\%$, the weight losses can be related to the formation of oxides. In Fig. 1 prepared samples (A, B and C) shows the DTA curves while the samples (A, B and C) elucidate TGA curves with different concentration of substituted ions respectively. It is observed that family of DTA curves reflect two exothermic and endothermic prominent peaks. The endothermic peak at $75^\circ C - 138^\circ C$ is related to the excretion of deposited water while the exothermic peak close to $80 - 100^\circ C$ is related to the crystallization temperature. Moreover, it is noteworthy in the family of TGA curve pattern which becomes linear near from $700^\circ C - 1000^\circ C$ which indicates that no further weight loss is done and starting of the formation of nano-crystalline spinel ferrite. Three different TGA curves which represent different concentration of the prepared samples, shows almost 81% weight loss in all the samples.

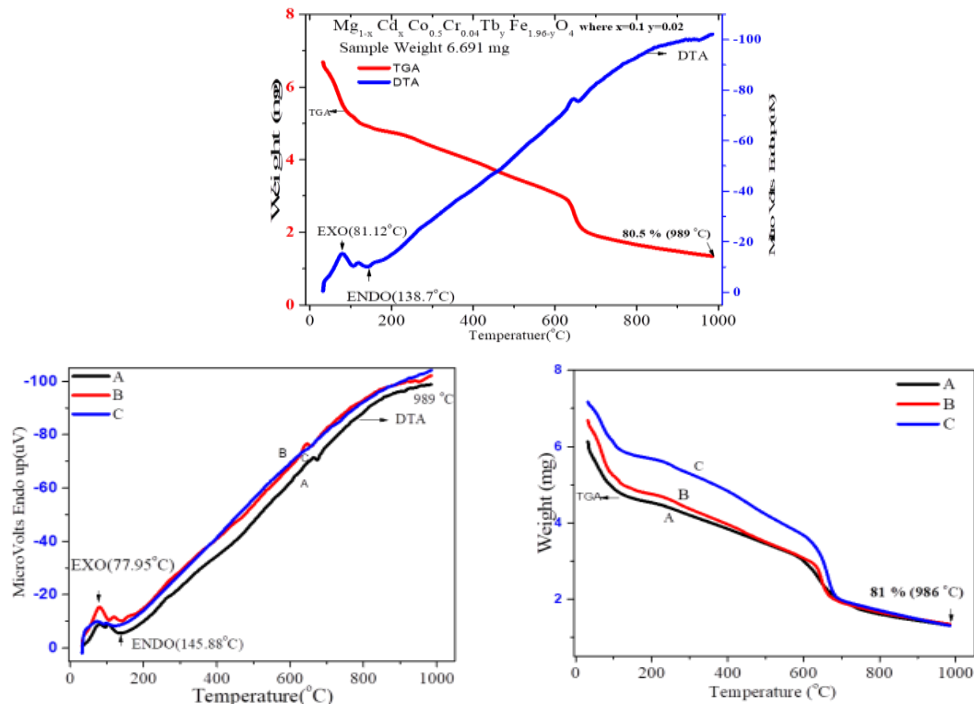


Fig. 1. TGA/DTA curves of the co-substituted (Cd^{2+} , Tb^{3+}) ions for Mg-Co-Cr powder.

Fig. 2 shows the represented sample, image of the micrograph exhibit well-defined shape. An average grain size is calculated by line intercept method it was found about in micrometer range. Such a behavior could be explained in the light of crystal growth process in a solution which depends on various factors; (i) the molecular concentration of the material approaching the surface of the tiny crystal during the growth process; (ii) the site preferences of the cations in the ferrite system; (iii) the local temperature is normally higher than the solution temperature due to the liberation of latent heat at the surface. The surface temperature affects the molecular concentration at the surface of the crystal and, hence, the crystal growth rate [8]. Moreover in the Fig. 2 also revealed energy dispersive X-ray spectra of the investigated samples. The required oxide materials were observed after the chemical reaction from these spectra. In this way the final product confirm that most of the undesired precursor materials like nitrates ions have been completely removed. The spectra demonstration the different orbital states of Mg, Co, Cd, Cr, Tb, Fe and O which proposes that the observed ratio of all the atoms is close to the reported values. The Cd at high temperature weight more than 30% reduced due to volatile behavior which is confirmed according to cited by reference [10].

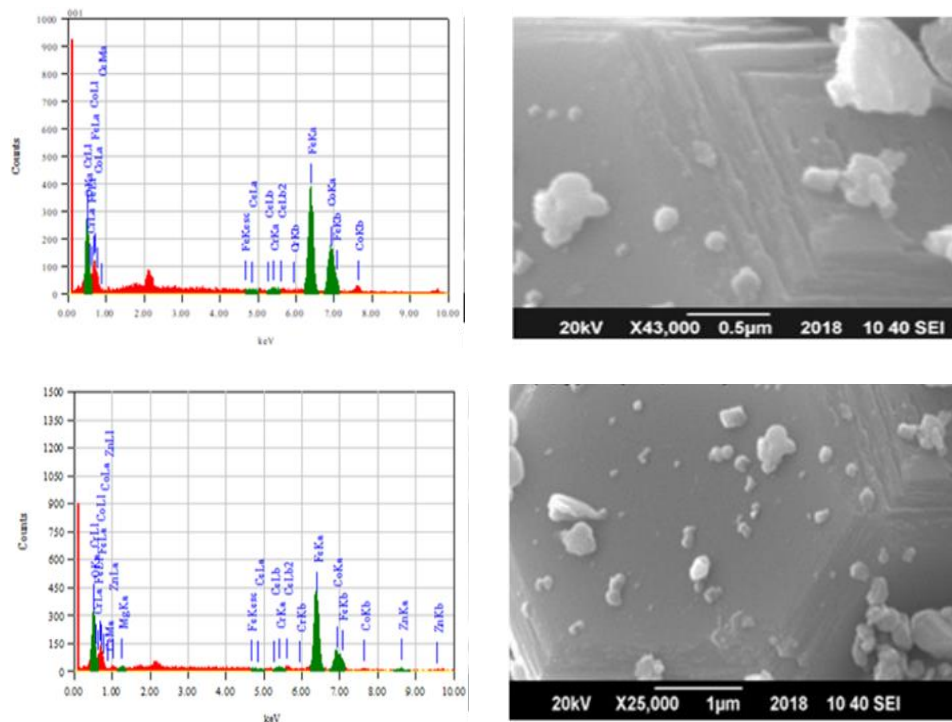


Fig. 2. EDX spectrum and SEM images of co-substituted (Cd^{2+} , Tb^{3+}) for Mg-Co-Cr-ferrite (x, y) = (0.4, 0.08).

The dc resistivity of spinel ferrites were calculated at room temperature by the use of Eq. (1). In the composition of the spinel ferrites, Mg^{2+} have a tetrahedral site instead of Fe ions appeared at A site and B site on the other hand (Cr^{3+} , Tb^{3+}) ions occupies the place of Fe ions B-site, hence the Fe ions decreases. The dc resistivity of spinel ferrites is actually substitution dependent of electrons in Fe^{3+} and Fe^{2+} at both sites. Hence electron hopping decreases in Fe^{2+} and Fe^{3+} ions. At last, the trend of resistivity show is increased ($1.15 \times 10^7 \Omega \text{ cm}$ - $6.88 \times 10^7 \Omega \text{ cm}$) with the increase in co-substituted (x, y) = (Cd^{2+} , Tb^{3+}) contents due to deficient iron ions at (B) site. Such a similar behavior reported by Farid *et al* [11] in $\text{MgPr}_y\text{Fe}_{2-y}\text{O}_4$ spinel ferrites. In the case of drift mobility, the obtained values fall in the range ($5.45 \times 10^{-11} \text{ cm}^2 \text{ V}^{-1} \text{ s}^{-1}$ - $6.74 \times 10^{-12} \text{ cm}^2 \text{ V}^{-1} \text{ s}^{-1}$) respectively. Moreover, in the conduction phenomena cobalt Co^{2+} ions play a dominant role as compared to other divalent ions in the spinel ferrites. The Co^{2+} ions also preferred to occupy at octahedral-site, consequently the number of hopping electrons decreases and increase in the electrical resistivity might be due to the conversion of Co^{2+} into Co^{3+} during the process of annealing and follow the exchange interactions. This provides a strong experimental evidence for the existence of small polarons and the hopping process [12]. Fig. 3 demonstrates an inverse relationship between drift mobility and electrical resistivity. The activation energy (E_a) of these charge carriers (electron and small polarons) is calculated by the relation [13];

$$E_a = 0.198 \times 10^{-3} \frac{d(\log \rho)}{d\left(\frac{1}{T}\right)} \quad (12)$$

where ' ρ ' is the resistivity, 0.198×10^{-3} is constant, k_B Boltzmann constant. The activation energy is increasing in the range (0.42 eV - 0.47 eV) in conduction. Rezlescu [14] reported that rising of the activation energy corresponds to the positioning of substituted cations at B sites. The increasing trend in the electric resistivity is due to the localization of Fe^{2+} ions. The obtained results of the samples showed that material has high electrical resistivity and activation energy while found low drift mobility.

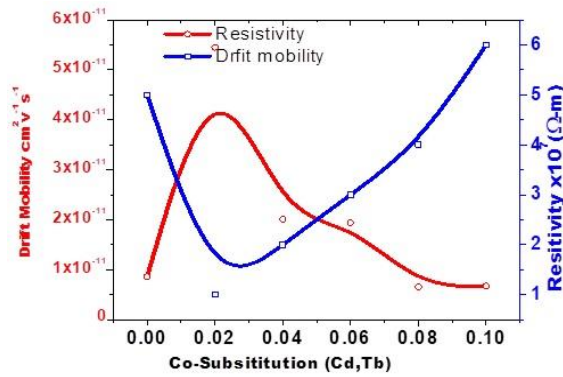


Fig. 3. DC-resistivity and drift mobility of co-substituted (Cd^{2+} , Tb^{3+}) for Mg- Co-Cr-ferrite system.

Dielectric response, generally in the ferrites samples count on microstructure, synthesis techniques, time and temperature for sintering, metal cations those are present both sites as well as the chemical composition [15]. Actually these behaviors of ferrites are considered as the frequency function and give comprehensive data about dielectric polarization mechanism as well as patterns of localized charge carriers [16]. Fig.4 illustrates the variation of the real part (ϵ') of dielectric constants by the variation of the frequency. It can be observed that with increase in frequency, real (ϵ') parts decrease first at a certain point then stop to decrease and get a constant value which shows the typical ferrite behavior [17]. In low frequency region, the values of dielectric constants (ϵ') are found high, this is due to the dominance of factors such as the vacancies of oxygen, divalent positive ions of iron, grain boundary defects, the interfacial dislocation and pile ups and voids etc.[18]. It was observed that Koop's theory as well as Maxwell-Wagner model is correlated to a point which states inhomogeneous two-layered dielectric structure which is a major reason for polarization of the space charge. It is also noticed that the doping of Tb^{3+} contents in spinel ferrites have a significant effect of dielectric constant due to local displacements and exchange electrons Fe^{2+} and Fe^{3+} play a key role in the production of dielectric polarization as well as the conduction procedure. Ions with larger ionic radii (Tb^{3+}) prefer to occupy octahedral sites [19]. As there is an increase in the doping of rare-earth (Tb^{3+}) ions, resistance of electronic exchange occurs between Fe^{2+} and Fe^{3+} which tends to significant decrease in values of dielectric parameters (ϵ') [20]. In terms of activation energy dielectric constant behaves opposite to the electrical resistivity. From the behavior of synthesized samples, it is concluded that it is useful especially for high-frequency applications due to high dissipation factor corresponds to lower dielectric parameters [21].

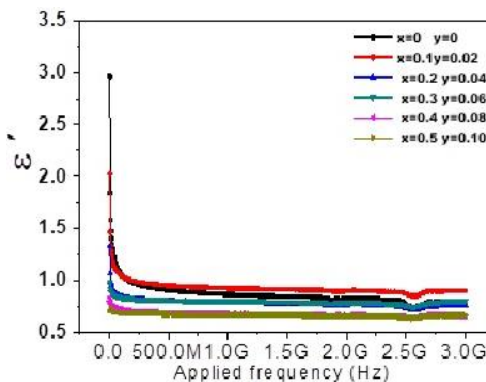


Fig. 4. Plots of dielectric Constant (ϵ') versus as a function of frequency of co-substituted (Cd^{2+} , Tb^{3+}) for Mg- Co-Cr-ferrites.

Fig. 5 interprets the dependence of the dielectric loss on the frequency in tangent $\tan(\delta)$. The value of $\tan(\delta)$ depends on different factors such as stoichiometry, homogeneity of structure

as well as sintering temperature of specimen etc. It is important to note that with increasing (Cd^{2+} , Tb^{3+}) concentration tangent get decreased. In low frequency region, hopping frequency of electrons among Fe^{2+} and Fe^{3+} ions present at octahedral sites, adjacent to each other. Maximum loss is because electrons strictly follow the field path. At the same time in low frequency region, tangent ($\tan\delta$) is at highest point and gets decreased in region of high frequency. Hence it can be assumed that in low frequency region, energy loss is high, so for hopping process charge carrier needed higher amount of energy resulting in higher loss. While in high frequency zone, exchange of electrons hopping frequency in Fe^{2+} and Fe^{3+} ions do not follow the applied field after a certain specific value of the critical frequency, that's why loss is minimized [22]. On the other hand, due to low energy loss in the zone of high frequency, energy requirement for the process of hopping is minimum for charge carriers. Specifically for this case, the synthesized ferrites have both the conducting and at the same time poorly conducting grain boundaries. In the low frequency region thin insulating grain boundaries are more effective, moreover conducting grain boundaries are in the high frequency region. Conductivity of material is related to the dielectric losses of the materials. Materials with high conductivity exhibits higher losses and vice versa [23].

Fig.5 shows that for the high frequency range especially above 2.7 GHz, many resonant peaks are found which clearly depicts the applied characteristics of the dielectric loss tangent. Reason behind this is undamped dipoles [24]. Maximum Dielectric losses constrained to the following conditions: $\omega_{max}\tau = 1$ where, $\omega_{max} = 2\pi f_{max}$ and (τ) = Relaxation time 'p' = jumping probability per unit time for the ionic/interfacial /electronic polarization. Both relaxation time and 'p' are related by the relation as; $\tau = \frac{1}{2\pi f_{max}} = 2p (f_{max} \alpha p)$. Ferromagnetic resonance can be elucidated on the basis of relaxation process by the Debye which both applied frequency and rate of hopping of electrons from Fe^{2+} to Fe^{3+} are approximately becomes equal to each other. Maxwell-Wagner prepared a comprehensive model to prove that abrupt decrease by the application of lower frequencies produces because of ferrites structure which is highly layered and non-homogeneous, that in returns produces dielectric behavior, which is also totally in accordance with the phenomenological theory of Koop [25]. Grains having lower resistance are very affective when the frequencies are very high. Low polarization of material at this point causes a decrease in dielectric constant. Many researchers observed the same findings. Grain boundaries' role becomes very effective at low frequencies [26]. Grain boundaries act as an insulator in the separation of grains. Applied field helps in charge carrier movement. Charge carriers' alignment on grain boundaries is carried out with the help grain boundaries having large hindrances. The values of dielectric constants increase due to charge polarization in space which is result of free charges at grain boundaries [27].

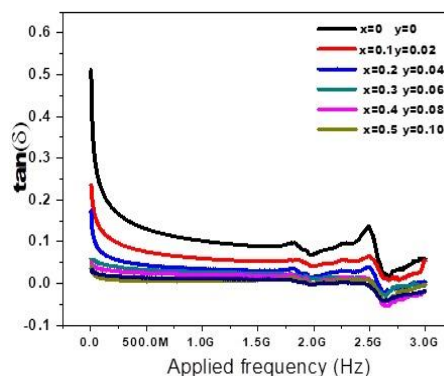


Fig. 5. Plots of dielectric loss tangent ($\tan\delta$) versus as a function of frequency.

Fig. 6 shows the permittivity spectra with its real and imaginary parts, which indicates a low dielectric constant and a very low dielectric loss. The obtained results are attributed to the structural and dielectric properties of heterogeneous ferrites resulted from interfacial polarization and corresponding relaxation.

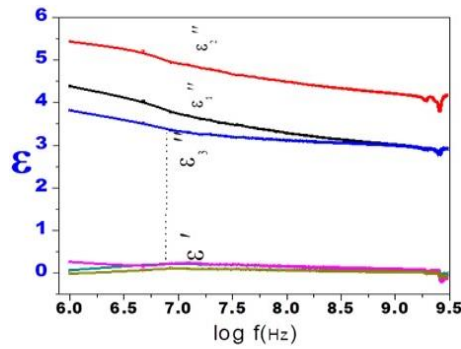


Fig. 6. Complex permittivity versus as a function of $\log(f)$ frequency.

The plot between ac conductivity versus frequency is given in Fig. 7. It was studied that the ac conductivity increases in the low frequency region however at higher range of frequencies it exhibits the dispersion behavior. To explain the behavior of ac conductivity, one can use the theory of Koop's and Maxwell-Wagner model. According to these, the ferromagnetic materials are composed of the grains that are conducting, whereas the grain boundaries are non-conducting thin layers. In the light of these, the obtained values of ac conductivity in the low frequency domain suggest the grain boundary behavior, whereas, at higher frequencies, due to the conductivity of grains, the dispersion is observed.

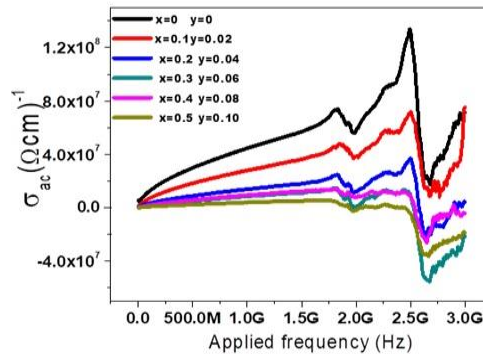


Fig. 7. Plots of variation ac-conductivity versus as a function of frequency.

Fig. 8 (a-b) shows the plot between $\log(\sigma)$ and $\log(\omega)$ in which amount of ac conductivity raised with the increase frequency of applied field. The increase this frequency increases the frequency of hopping in the exchange of Fe^{2+} and Fe^{3+} and as a result the conductivity increases. For evaluating the ions vibration of their spinel conduction sites joined with the hopping to the neighboring sites through energy constraints of E_{AC} (AC activation energy), the following expression is used; $\tau_{o(T)} = \tau_{\infty} \exp\left(\frac{E_{ac}}{K_B T}\right)$ where τ_{∞} represents the reciprocal to the frequency applied of the present ions as well as the (τ_0) represents the relaxation time in terms of ion-hopping. Normally, for DC conductivity the activation energy will be larger than the energy barrier and is given by [28] $E_{dc} = \frac{E_{ac}}{(1-n)}$. Increased interactions in the moving ions result in increased values of 'n'. Moreover increased value of 'n' shows increase cooperation during the ion-hopping process [29]. The higher concentration of rare earth content, the greater is the disorder in the structure. This is due to the different sizes of the host and dopant ions at various spinel sites. The increased ion-ion interactions may result in the higher values of 'n' thereby resulting in energy penalty which in turn is imposed on DC or long range conductivity resulting from this correlation. This reveals increasing rate that occurs in E_{DC} and E_{AC} (larger value of n).

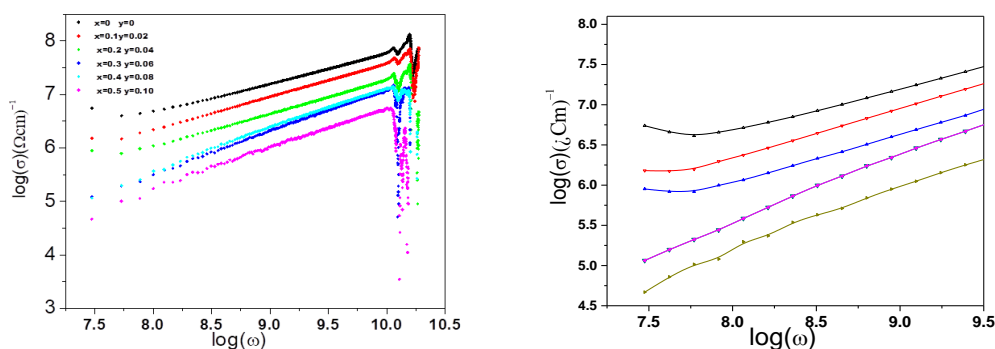


Fig. 8. (a-b) Plots of variation AC-conductivity $\log(\sigma_{AC})$ versus as a function of $\log f(\omega)$.

Impedance spectroscopy is important in the analysis of all the contributions (electrode/electrolyte interfaces, grain and grain boundaries) to resistances in the flow of current through a dielectric medium. It's a complex function with magnitude and phase angle [30].

Fig. 9 shows the value of magnitude Z reduces by increasing the frequency, representing increase in the values of AC conductivity. It is also confirmed that it has a smallest grain-boundary resistance and highest conductivity which might be due to large grain size and smaller area of the grain boundary. The hopping of charge carriers between two spinel sites is enhanced at high frequencies leads to high values of impedance. The impedance shows the reciprocal trend with AC conductivity.

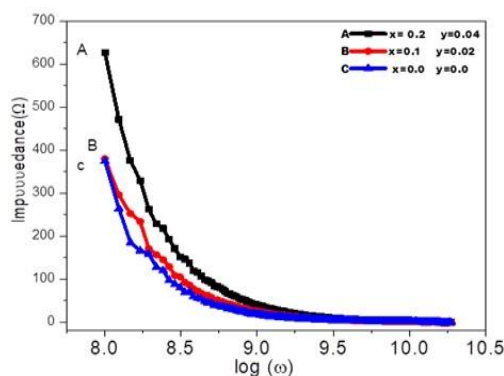


Fig. 9. Impedance versus as a function of $\log(\omega)$.

Figs. 10 show variation of the real parts of electric modulus against frequency which is a power full procedure to study relaxation phenomenon in the material. In order to study the frequency dependences of the interfacial polarization effect, electrical modulus can be used to generate electric charge accumulation around the ceramic particles by displacing relaxation peaks. The Maxwell-Wagner model provides information for the behavior of complex conductivity in heterogeneous systems with two or more phases [31]. The value of real modulus was smaller in lower frequency region and enhanced with the increase of applied field frequency and approached toward a maximum constant value at still higher frequencies, which might be due to a lack of restoring force responsible for movement of charge carriers due to the influence of an applied electrical field. The resonance peaks appeared when the jumping frequency Fe^{2+} and Fe^{3+} electrons was equal to the frequency of applied ac field [32].

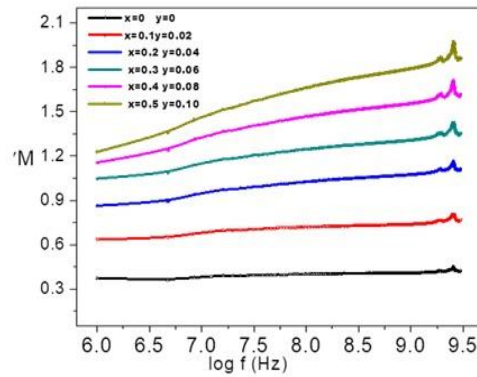


Fig. 10. Variation in real part of electric modulus versus as a function of frequency.

There are two methods through which AC data can be explained. As the capacitance is changed, the relaxation phenomenon is also changed then impedance plane plot is useful. If the relaxation phenomenon is sensitive to resistance, then electric modulus plane plot is beneficial [33]. In the present case, no satisfactory results have been obtained by impedance plots; however complex modulus is much favorable and easily explained the relaxation phenomenon. Fig. 11 shows the Nyquist plot (Cole–Cole) in the (Cd-Tb) spinel ferrites. The left side representing the lower frequencies of the given stands semicircle in the grain resistance on the other hand grain boundary as a result of frequencies [34] on the other hand whole grain resistance having higher frequency appeared at right side [35]. Substitution has less difference in terms of grain resistance, contrarily resistance of grain boundaries increases considerably. Higher the contents of Tb^{3+} higher will be the resistance of grain boundary. The hopping mechanism is actually strong conduction mechanism, this might be an easy way to transfer electron in Fe^{2+} to Fe^{3+} and vice versa. When the substitution of Tb^{3+} contents by the use of Fe and decrease the transfer of Fe^{2+} and Fe^{3+} . Resistivity values of ferrite ions fluctuate when there is a change in composition and grain boundary. Clearly the Tb^{3+} doping affects the resistance of grain boundary. Impedance conductivity at grain boundaries are represented by the formation of high resistance regions. The dielectric constant and resistivity were determined by the high resistance of the grain.

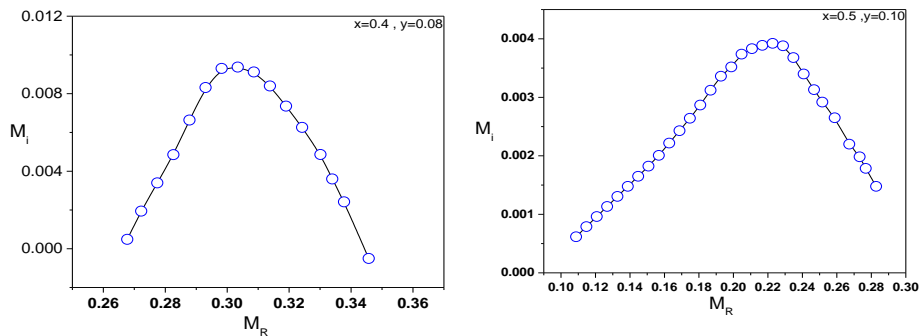


Fig. 11. Plot of Cole-Cole co-substitution (Cd^{2+} , Tb^{3+}) for Mg-Co-Cr-Fe-O ferrite system.

4. Conclusion

A series of co-substituted (Cd, Tb) spinel ferrites, has successfully been synthesized using sol-gel method. In thermal analysis, TG/DTA curves revealed the decomposition mechanism of the precursors among representative samples and eliminated the decomposed organic compounds near the temperature of 600 °C. Above this temperature, behavior of curves became linearly flat, which showed that metal oxide phase has developed. Scanning electron microscopy (SEM) revealed the material morphology and size of grain was found 0.44 μm with definite crystalline cubic shape, which helps to reduce the complex permeability. Observed behavior of various

parameters of dielectric by varying frequency in specific ranges confirms the Maxwell-Wagner polarization model. The main reason behind the observed conductivity mechanism is due to hole and electron hopping. The ac conductivity, in a wide range of frequencies, shows a similar behavior to semiconductors. Change in exponent 'n' depends upon composition and confirmed that hopping charges produce the conduction. With these characteristics, the synthesized ferrites is a potential candidate for applications such as switching and microwave devices and electromagnetic attenuation materials.

Acknowledgements

The author is thankful to Higher Education Commission (HEC) of Pakistan for providing financial support to carry out this work under IRSIP scholarship.

References

- [1] M. Gabal, Y. Al Angari, H. Zaki, J. of Magn. and Magn. Mater. **363**, 6 (2014)..
- [2] T.-H. Ting, K.-H. Wu, J. of Magn. and Magn. Mater. **322**(15), 2160 (2010).
- [3] M. Anis-ur-Rehman, G. Asghar, J. of Alloy. and Comp. **509**(2), 435 (2011).
- [4] N. Rezlescu, E. Rezlescu, Solid State Communications **88**(2), 139 (1993).
- [5] C. B. Kolekar, P. N. Kamble, A. S. Vaingankar, J. of Magn. and Magn. Mater. **138**(1), 211 (1994).
- [6] A. Pradeep, G. Chandrasekaran, Materials Letters **60**(3), 371 (2006).
- [7] G. Mustafa et al., J. of Magn. and Magn. Mater. **387**, 147 (2015).
- [8] E. Barsoukov, J. R. Macdonald, 2005: John Wiley & Sons.
- [9] N. Rezlescu, E. Rezlescu, Physica Status Solidi (a) **23**(2), 575 (1974).
- [10] N. Amin et al., Digest Journal of Nanomaterials and Biostructures **11**(2), 579 (2016).
- [11] H. M. T. Farid et al., Cera. Inte. **43**(9), 7253 (2017).
- [12] I. Ali et al., J. of Magn. and Magn. Mater **362**, 115 (2014).
- [13] M. A. Iqbal et al., Cera. Inte. **39**(2), 1539 (2013).
- [14] A. Thakur, P. Mathur, M. Singh, J. of Phys. and Chem. of Solids **68**, 378 (2007).
- [15] E. Rezlescu et al., Crystal Research and Technology **31**(3), 343 (1996).
- [16] K. K. Bharathi, C. Ramana, J. of Mate. Rese. **26**(4), 584 (2011).
- [17] E. Pervaiz, I. Gul, Inter. J. of Current Engg. and Technology **2**(4), 377 (2012).
- [18] N. Rezlescu, E. Rezlescu, Physica Status Solidi (a) **23**(2), 575 (1974).
- [19] D. Ravinder, P. V. B. Reddy, Materials Letters **57**(26), 4344 (2003).
- [20] Y. Kolekar et al., Journal of Applied Physics **115**(15), 154102 (2014).
- [21] C. Murugesan, G. RSC Advances **5**(90), 73714 (2015).
- [22] M. J. Iqbal et al., J. of Magn. and Magn. Mater. **323**(16), 2137 (2011).
- [23] U. Shinde et al., Ceram. Inter. **39**(5), 5227 (2013).
- [24] A. Hudson, Marconi Review **31**, 43 (1968).
- [25] M. T. Farid et al., J. of Magn. and Magn. Mater. **422**, 337 (2017).
- [26] D. Carta et al., Journal of Physical Chemistry C **113**(20), 8606 (2009).
- [27] M. El Hiti, J. of Magn. and Magn. Mater. **164**(1-2), 187 (1996).
- [28] K. L. Ngai, S. . Martin, Physical Review B **40**(15), 10550 (1989).
- [29] K. Ngai, C. León, Physical Review B **66**(6), 064308 (2002).
- [30] K. Ngai, C. León, Solid State Ionics **125**(1), 81 (1999).
- [31] J. R. Macdonald, W. B. Johnson, Second Edition 1 (2005).
- [32] A. Farea et al., J. of Alloy. and Comp. **469**(1), 451 (2009).
- [33] Y. Bai et al., J. of Magn. and Magn. Mater. **278**(1), 208 (2004).
- [34] M. Chourashiya et al., Materials Chemistry and Physics **109**(1), 39 (2008).
- [35] I. Ali et al., J. of Alloy. and Comp. **579**, 576 (2013).